Korean J. Chem. Eng., 35(10), 2001-2009 (2018)
DOI: 10.1007/s11814-018-0106-9

pISSN: 0256-1115
eISSN: 1975-7220

Improvement of liquid fuel atomization for an internal engine using an auxiliary device

Jia Ping Feng*,‡, Sang In Choi*, Ho Seok Seo, and Young Min Jo*,†**

*Department of Environmental Science and Engineering, Center for Environmental Studies, Kyung Hee University, Yongin 17104, Korea
**EG Power Tec Co., Ltd., Suwon 16229, Korea
(*Received 16 October 2017 • accepted 24 June 2018*)

Abstract−Controlled atomization is essential for reducing soot emission in practical diesel engines. In this work, an auxiliary device called a FAD (fuel activation device) was inserted into the fuel injection line to induce cavitation in the diesel spray. The performance of the FAD was examined in terms of pollutant emissions in a field test as well as aerosol sizes in lab-scale experiments. Experimental results showed that FAD reduced the size distribution of injected droplets and decreased the fuel consumption rate and emission amounts of PM_{10}, CO, and NO_x by 42%, 50% and 13.4%, respectively.

Keywords: Fuel Activation Device (FAD), Diesel Engine, Fuel Atomization, Nozzle Injection

INTRODUCTION

Although diesel engines of heavy trucks and trains have been preferred due to their high fuel efficiency and power output, combustion of diesel fuel emits more nitrogen oxides (NO_x), particulate matter (PM) and carbon monoxide (CO) compared to gasoline [1-3]. Old vehicles are a critical emission source for urban air pollutants. In 2017, the Korea Environment Ministry began regulating vehicles registered before 2006 to implement a diesel car scrappage program [4]. Most developing countries are experiencing challenges from the significant amount of air pollution emitted by these heavy, old automobiles. One way to mitigate these harmful emissions is by using a diesel particulate filter (DPF), but most transport operators prefer not to use these devices because they decrease the output power.

In a typical diesel engine system, the fuel is injected into the engine chamber near the end of the compression stroke at a small crankshaft angle [5]. Then the fuel can be automatically ignited and combustion subsequently proceeds. The combustion determines the heat release rate, engine noise and pollutant formation. As the fuel aerosol absorbs heat energy from the compressed air, it burns, leading to the production of thermal energy [6,7]. Improved surface contact between the fuel droplets and air can increase the conversion rate of fuel chemical energy to mechanical energy via high efficiency combustion. Therefore, it is important for a fuel atomizing burner to optimize the mix ratio of fuel to air [8-10].

Nozzles are crucial parts of a fuel supply system, and the relationship between nozzle geometry and injection efficiency has often been investigated [11-13]. The nozzle structure determines the atomization effect and the acceleration of liquid fuel. The droplet sizes of the atomized fuel depend on the diameter of the nozzle orifice and the injection pressure [14]. Payri et al. [13] demonstrated that cylindrical nozzles tend to facilitate cavitation effects, while conical nozzles suppressed this phenomenon [13]. Cavitation plays an important role in the process in that liquid fuel forms fine droplets or bubbles in response to sudden changes in the flow direction and flow velocity due to changes in the static pressure [15]. Nurick [16] developed a phenomenological model to explain a cavitation effect that could improve the liquid atomization during the process of fuel atomization.

Various nozzle designs have been explored to improve the cavitation effect [17-19], and these works focused on mechanical improvements to form liquid droplets by cavitation through a new fuel activation device (FAD) (PATENT-2015-0021792). Our previous numerical study demonstrated that an FAD enhanced the cavitation phenomenon inside the nozzle and improved diesel atomization [20]. In the present study, we sought to further observe the function of the FAD in diesel atomization through lab tests as well as field tests. FADs have been considered for use in older and heavier vehicles such as heavy trucks, buses or trains to enhance atomization, since smaller fuel droplets result in improved combustion efficiency. A higher combustion efficiency equates to a reduction in fuel usage and fewer harmful emission.

THEORETICAL BACKGROUND

1. Fuel Cavitation through Nozzle Injection

Many researchers have investigated cavitation phenomena for liquid flow through nozzles [21-24]. Liquid fuel accelerates rapidly as it passes through narrow nozzle holes, as per the Bernoulli equation. The large gradient in the velocity results in a strong shear flow,

†To whom correspondence should be addressed.
E-mail: ymjo@khu.ac.kr
‡Current affiliation: Particle & Air Pollution Control Laboratory, Department of Environmental Science and Engineering, Kyung Hee University, Yongin 17104, Korea

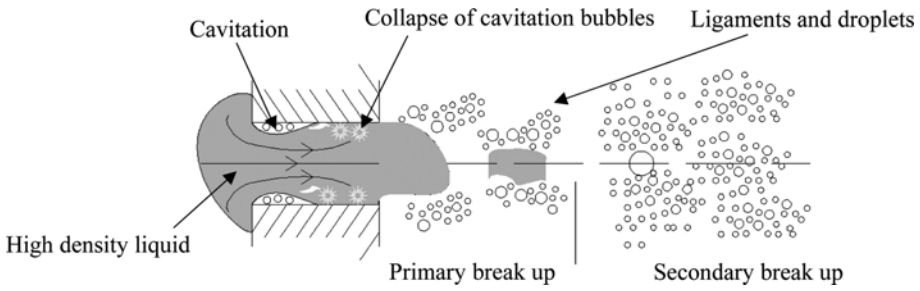

Fig. 1. General structure of liquid break-up process with cavitation (modified from ref. [28]).

and induces cavitation with a highly turbulent vortex. The intensity and spatial distribution of the cavitation zones depend on the nozzle geometry and pressure boundary conditions [25].

Liquid droplet break-up primarily occurs through disintegration of the coherent liquid into ligaments and large drops [26]. Large droplets are further broken into tiny droplets by aerodynamic forces due to the velocity difference between the droplets and carrier gas. The cavitating bubbles implode due to the increased static pressure as they approach the nozzle outlet. The turbulent kinetic energy of the jet injection sprays the disintegrated aggregated droplets into the combustion chamber. Thus, implosion of liquid droplets by cavitation is closely related to the position across the injection nozzle. Salvador et al. [27] presented a model to explain the atomization by correlating the dynamic behavior inside the injector with the turbulence. Fig. 1 is a basic model of diesel sprayed along the core flow path with the formation of bubbles and bubble break-up [28]. A new primary break-up model for diesel spray was presented with cavitation effects assuming that primary break-up occurred inside the nozzle [26]. In other words, the bubbles collapsed after cavitation providing extra energy for liquid deformation, which may contribute to the subsequent break-up of the sprayed liquid fuel in this work.

2. Fuel Activation Device (FAD)

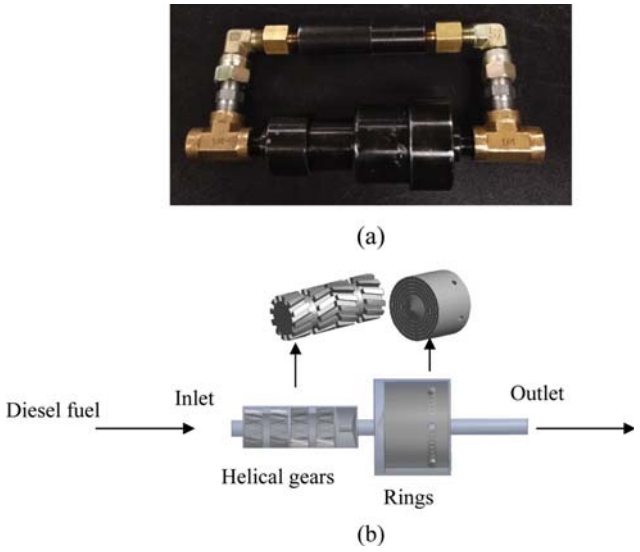

Fig. 2. Schematic structure of (a) test FAD and (b) 3D geometry of FAD.

The FAD presented in this work was designed to add the driving energy before the fluid reached the nozzle. Fig. 2 shows a schematic structure of the interior of the FAD used in this work. It was designed to provide pressurized diesel fuel with strong swirling turbulence. The spiral flow path based on helical gears adds some kinetic energy to the entering liquid fuel flow and facilitates atomization. The flow direction arbitrarily changes across the FAD. Six-larger rings rotate the entering flow and generate a strong vortex, which acts as resistance.

Cavitation also happens inside the FAD, including the inlet passage, the passage connecting helical gears with big rings and the outlet passage. As the flow moves on, cavitation bubbles collapse in these positions, and thus induce stronger turbulence and ultimately transfer more driving energy to the flow. Thus, the reduced forward pressure and high velocity of the flow increase the cavitation phenomena inside the nozzle. The fuel atomization at the injection nozzle can be enhanced to a certain extent with the increased kinetic force and the cavitation effects provided by the FAD.

MATERIALS AND METHODS

1. Simulation of FAD Internal Flow

To better understand the function of FAD, we conducted a simple simulation study of the flow behavior inside FAD. This study included axial velocity, pressure and cavitation and was conducted using a commercial computational fluid dynamics software for an injection pressure of 0.75 MPa.

2. Lab Scale Test

Fig. 3 is the overall schematic diagram of a test layout for fuel atomization and size analysis. A fuel pump (General Motor Company - Korea) was used to pressurize the diesel from the fuel tank (2) and deliver it to the particle sizer with or without going through the FAD. A pressure gauge (5) was used to measure the differential pressure before and after the FAD (4). To stabilize the fuel injection, the fuel pump was run for more than 20 seconds before beginning measurements using a particle size analyzer (9) (Mastersizer 2000, Malvern Instruments Ltd, United Kingdom) with a detection range from 0.02 to 2,000 μm. Aerosol size was repeatedly measured more than five times, with an experimental uncertainty of less than 4.57% as the spray was injected across the dark box of the laser device. The obtained data were then analyzed, focusing on the median size as well as the overall distribution. A vacuum pump (10) was placed 10 cm from the laser center; this location minimized the measurement errors, and the released fuel droplets

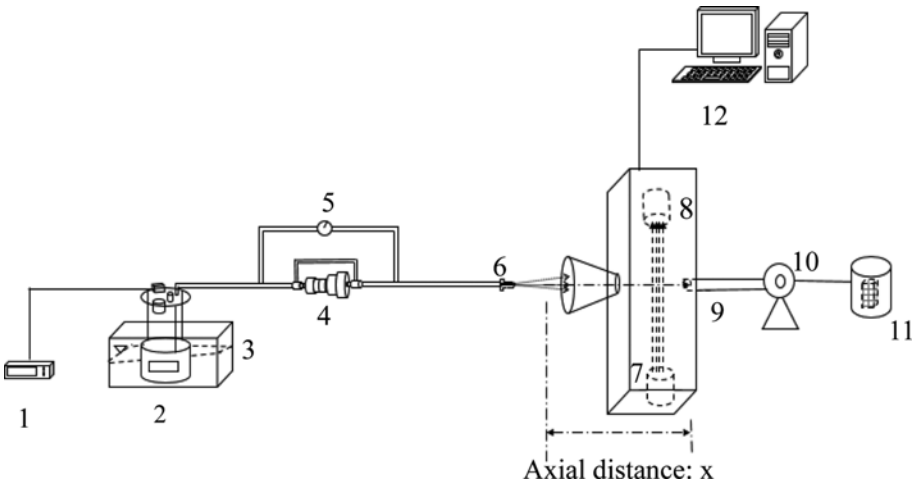

Fig. 3. Schematic diagram of experimental layout for spray test.

1. Power adapter
2. Fuel tank
3. Fuel pump
4. FAD
5. Pressure gauge
6. Nozzle
7. Laser source
8. Laser receiver
9. Particle analyzer
10. Vacuum pump
11. Filter bunker
12. Data acquisition PC

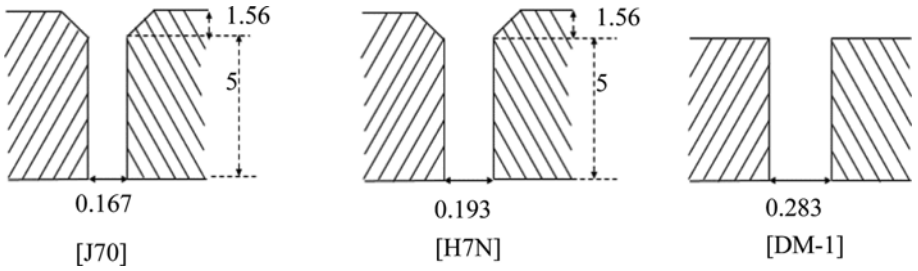

Fig. 4. Configuration of test nozzles (Unit: mm).

Table 1. Test fuel diesel properties

Property	Value
Density (kg/m^3)	830
Viscosity [kg/(m·s)]	0.00224
Vapor pressure (MPa)	0.00128
Surface tension (N/m)	0.031

Table 2. Experimental conditions

Hole diameter (mm)	0.167, 0.193, 0.283
Injection pressure (MPa)	0.4-0.75
Ambient pressure (MPa)	0.1
Ambient temperature (K)	293

were then collected in a filter bunker (11).

The fuel atomization in this work was at a lower injection pressure than actual car engines to precisely examine the cavitation effect inside the nozzles, as has been done in many preliminary studies [29-33].

As schematically illustrated in Fig. 4, three nozzles with different geometries were tested in this work. Test nozzles J70 and H7N (Danfoss Company, Denmark) were designed with the same cylindrical cross-section but different outlet orifice diameters of 0.193 and 0.167 mm, respectively. With regards to cylindrical nozzles, a smaller hole diameter results in smaller original droplets ejected from the nozzle and will also lower the mass flow rate [34]. A commercial diesel nozzle (DM-1) for a passenger car (Trax, Chevrolet. GM) with an orifice of 0.283 mm was also used. The test diesel was procured from a local gas station (GS Caltex, Korea), and its properties are summarized in Table 1. Other experimental conditions are presented in Table 2. Diesel fuel was injected at a pressures from 0.4 to 0.75 MPa under ambient lab conditions.

3. Field Test

Fuel atomization by FAD was expected to reduce the fuel consumption for a similar vehicle power output. This has been experimentally confirmed with the operation of heavy trains in Mongolia, which showed lower emission of black soot with a previous FAD model [35].

To determine the effect of the FAD on air pollution, we conducted field tests in a steady condition without dilution in a 1 ton truck (Bongo 3, KIA Motors, Korea) with three replicates. The field test equipment consisted of an engine, an FAD, an air flow rate meter, and an exhaust analyzer (KM-9106, KANE, U.K) to analyze exhaust pollutants such as fine dust (PM), nitrogen oxides (NO_x) and carbon monoxide (CO). Fuel efficiency was evaluated according to five driving load steps from idle to 4 speeds, 30, 60, 80 and 100 km/h. Exhaust gas was analyzed for 20 minutes after stabiliza-

Table 3. Field test conditions

Engine type	L4 2.5
Fuel type	Diesel
Absolute temperature (K)	295.16
Relative humidity (%)	76
Ambient pressure (kPa)	101.325
Exhaust gas flow rate (m^3/min)	4.14
Oxygen concentration (%)	14.8

tion at each speed.

RESULTS AND DISCUSSION

1. Numerical Simulation of FAD Internal Flow

One of the main atomization mechanisms in liquid fuel injection is the cavitation effect, and it can be characterized by cavitation number as defined in [48]:

$$\sigma = \frac{P_{back} - P_{static}}{1/2\rho v^2} \quad (1)$$

where P_{static} denotes the static pressure inside the nozzle, P_{back} denotes the chamber pressure, ρ denotes the liquid density, and v denotes the inlet velocity of the diesel flow into the nozzle. Our previous study showed that cavitation occurred when the cavitation number was lower than a critical value and gradually developed as the number decreased. Higher cavitation numbers resulted in smaller droplets [36].

A simulation study was carried out to determine the effect of the FAD on the cavitation in the nozzle as a function of pressure and velocity for a flow travelling time of 0.6 ms. As shown in Figs. 5 and 6, the pressure of the diesel flow into the nozzle decreased while the flow velocity increased. This indicates that cavitation effects are more developed for a lower cavitation number inside the nozzle. In other words, the flow velocity from the FAD to the nozzle

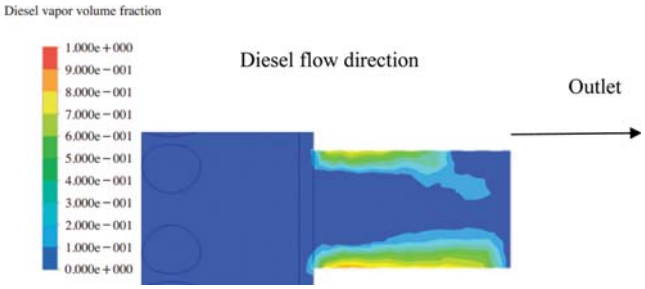

Fig. 7. Diesel volume fractions with cavitation effect in the FAD outlet region.

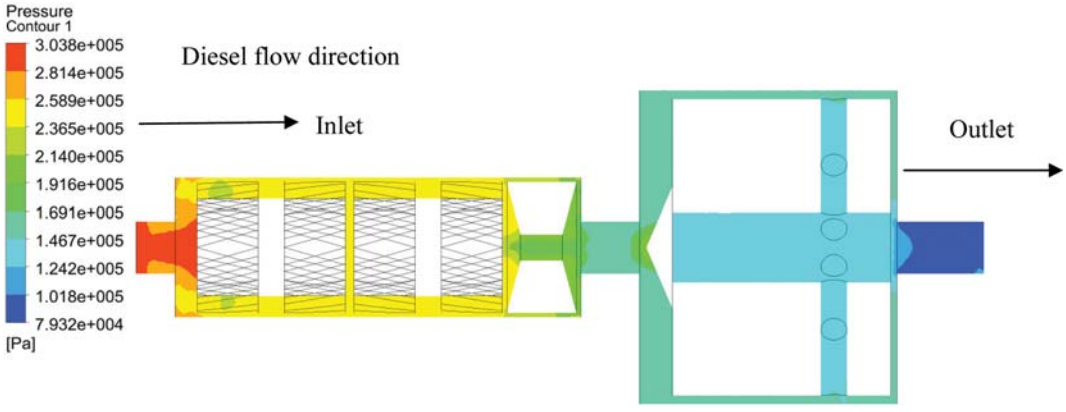

Fig. 5. Static pressure distribution across the FAD.

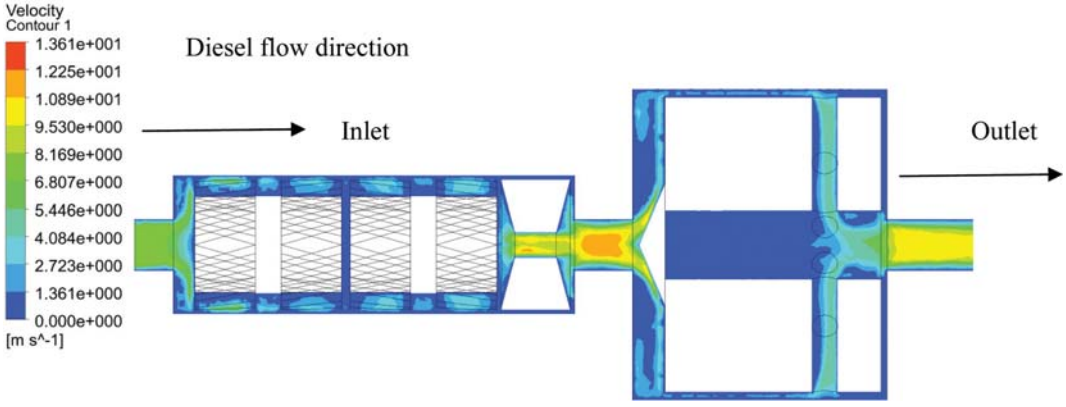

Fig. 6. Velocity distribution inside the FAD.

increased due to the collapse of the cavitation bubbles as seen in Fig. 7. Another study by Choi [20] further demonstrated the effect of FAD on cavitation development inside the nozzle.

Fig. 5 also shows the decrease in pressure drop through the FAD, from 0.3 MPa upstream to 0.08 MPa downstream, when the injection pressure was 0.75 MPa. The velocity shown in Fig. 6 increased proportionally with the decreased pressure, while the mass flow rate was almost the same in the nozzle with and without the FAD. A more detailed flow distribution across the outlet of the FAD is shown in Fig. 7.

2. Characterization of Fuel Atomization

The fuel supply flow rate from the fuel pump was 1.5 L/min with or without nozzles or FAD. This demonstrates that there was no loss in fuel due to the installation of the mechanical auxiliary devices.

2-1. Size Distribution of Atomized Droplet

The Sauter mean diameter (SMD) is the ratio of the aerosol volume to its surface area and defined in Eq. (2) [28], where n_i is the number of X_i diameter droplets. SMD reflects the degree of diesel atomization. In this study, SMD measurements were performed using a laser diffraction particle sizer at various distances from the fixed injection point over five repetitions. The particle size was measured in real time as a function of the axis position to determine if the FAD influenced the size development of the injected droplets along the axial flow path as described previously [37-39]. Axial distance (x in Fig. 3) was defined as the distance from the test nozzles to the laser diffraction measuring point. Injection positions based on axial distance were 7, 9 and 11 cm for each nozzle. Injected fuel droplets were sufficiently atomized at these distances, as was apparent based on visual observations.

$$SMD = \frac{\Sigma_i n_i X_i^3}{\Sigma_i n_i X_i^2} \quad (2)$$

Fig. 8 shows the effect of the FAD on liquid fuel atomization. Regardless of nozzle type, FAD reduced the sizes of the atomized fuel droplets to a certain degree. The SMD did not consistently depend on the axial distance from the nozzle tip to the measuring point. Nevertheless, nozzles H7N and J70 (with the tapered tips) showed that size decreased as the distance increased for the cases without the FAD. This implies that the atomized fuel was widely dispersed in the measuring box, resulting in a lower probability of coagulation by less frequent contact. In addition, the structures of these nozzles also promoted break-up of the droplets based on air shear and particle surface tension. The SMD of H7N was always larger than that of J70 under the same axial distance without the FAD, because H7N had a larger hole diameter and ejected larger

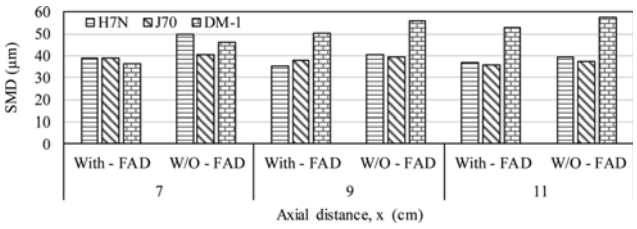

Fig. 8. SMD distribution of atomized diesel fuel for each nozzle with and without FAD for various injection positions.

intrinsic droplets from the nozzle tip [14]. Thus, secondary break up generated large droplets even under the same ambient conditions. In contrast, nozzle DM-1 showed increased droplet size with increasing distance (x=9, 11 cm) because the straight injection might have caused more frequent collisions and coagulation as the fuel exited the nozzle; thus, larger droplets appeared from 7 to 11 cm as distance increased and the dispersion also became wider.

The FAD did not change this tendency even though there was an obvious decrease in size. For H7N, FAD decreased the SMD by 21.82%, 13.44%, and 5.44%, corresponding to distances of 7, 9, and 11 cm, respectively. The decreasing rate of the size was more significant at closer injection points (e.g., 7 cm). A much lower effect was seen in nozzle J70: 3.93% to 3.33%. The decrease in size for nozzle DM-1, which is used in commercial cars, was obvious at 21.40%, 10.10% and 8.14% for 7, 9 and 11 cm, respectively.

The uniformity and divergence of atomized fuel droplets were reviewed based on the relative span factor (RSF) of the droplet size as defined in Eq. (3) [40]:

$$RSF = \frac{D_{(v,\,0.9)} - D_{(v,\,0.5)}}{D_{(v,\,0.1)}} \quad (3)$$

Here, the values of RSF indicate the dispersion condition of aerosols in the combustion chamber of the diesel engine. A more uniform spray is obtained when the RSF is close to 1 [41]. Thus, the spatial distribution of the atomized fuel is estimated in terms of the injection conditions [37,42]. $D_{(v,0.9)}$, $D_{(0,0.5)}$ and $D_{(0,0.1)}$ represent the cumulative aerosol sizes which occupy 90%, 50% and 10% on a volume basis. Evaluated values of RSF for three nozzles at different axial distances are summarized in Table 4. The RSF of DM-1 tended to decrease with the addition of FAD, revealing more uniform droplets. Such a distribution could be due to a considerable decrease in large and medium particles. H7N showed the opposite result, and the J70 results were somewhat inconsistent. So, the size distribution of atomized fuel from the initial position showed different trends depending on the nozzle type. There must be an optimum injection position along the axial distance for each nozzle configuration. Nevertheless, DM-1 showed a homogeneous distribution of atomized droplets regardless of axial position.

Fig. 9 shows a more precise cumulative volume fraction of all atomized droplets when using the FAD for different nozzles. Dot-

Table 4. Relative span factors of each nozzle with and without FAD at different injection distances

Nozzle types	Axial distance (cm)	RSF	
		With-FAD	Without-FAD
J70	7	1.21	1.21
	9	1.31	1.24
	11	1.17	1.27
H7N	7	1.24	1.03
	9	1.35	1.16
	11	1.28	1.24
DM-1	7	1.46	1.58
	9	1.43	1.55
	11	1.56	1.58

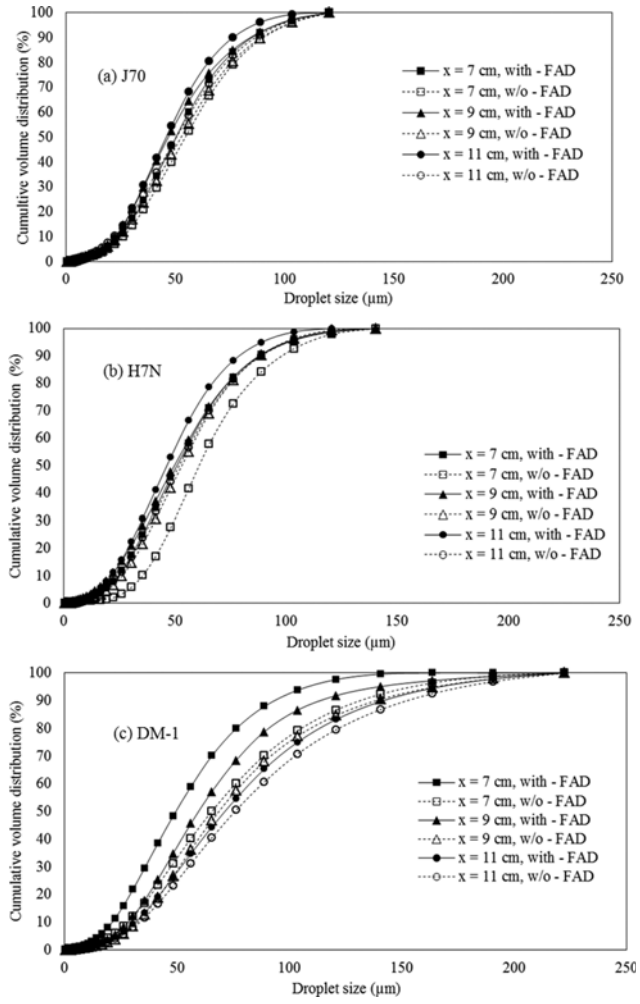

Fig. 9. Cumulative size distribution of atomized droplets with and without FAD for different axial distances and nozzle types.

ted lines indicate the case without the FAD, and the solid lines shown below indicate data with the FAD. This result implies that the FAD decreased the atomized fuel size. While the distribution spread out to over 200 μm for DM-1, droplets injected from J70 were distributed up to 120 μm. That was because different nozzle configurations developed different cavitation mechanisms [17]. Flow patterns varied with injection nozzle, volumetric flow rate and internal flow pattern, and the subsequent break-up of the droplets was different. Fig. 9 clearly shows that, at the same axial distance, the curves with the FAD shifted to the left relative to the data without FAD. Thus, we concluded that the FAD reduced the average particle size, particularly for DM-1.

The effect of FAD on the atomization was more obvious for a short flow path, such as 7 cm, rather than 11 cm. This is because a more vigorous dispersion may occur while the droplets are traversing the longer distance. Chances of collisions increase, and the tendency of droplets to coalesce also increases. As the heterogeneity in particle size increased along the axial distance, the rate of coagulation increased; therefore, locations nearer to the nozzle had better atomization effects with the FAD [43].

2-2. Cavitation Effect with Injection Pressure

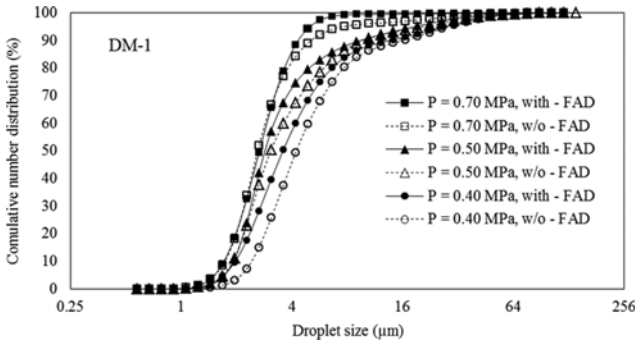

Fig. 10. Droplet size distribution with fuel atomization with and without the FAD for various injection pressure in a DM-1 nozzle.

Liquid atomization in a nozzle usually arises from cavitation in the nozzle or from the primary breakup of the liquid core depending on the Reynolds number. The atomized liquid fuel can be finely split again by secondary breakup through friction with air [44]. Since primary breakup contributes greatly to the final droplet size, the efficiency of the diesel engine has, in practice, been enhanced by a high injection pressure accelerating the liquid fuel flow or by utilization of cavitation effects [30].

In this work, installation of FAD was assessed by the investigation of microscopic droplet size. While the modern CRDI (common rail diesel injection) system adjusts the flow rate of the nozzle via electrical control in milliseconds [45-47], this study required a sufficient stabilization time of approximately 20 seconds at 6 bars because the liquid fuel had to pass through the FAD.

Fig. 10 shows the cumulative number fraction of droplets for different injection pressures at an axial position of x=7 cm for the DM-1 nozzle with a FAD. Here, the cumulative number basis was more effective for understanding fuel atomization because it directly shows the number of particles in each size range. At the same injection pressure, the droplet size curve shifted to the left after installation of the FAD. Thus, the effect of the FAD was more significant when operating at high pressure. Therefore, the cavitation of fuel droplets was most significant at 0.4 MPa in this work. Nevertheless, the injection pressure at the nozzle is a dominant parameter for determining the size distribution of the atomized fuel.

In practice, the reduction of the droplets implies vigorous cavitation or increased internal flow velocity [13,48]. Such behavior is apparently caused by the FAD. Accordingly, it can be concluded that the FAD enhanced the turbulence of the flow entering the nozzle and decreased the injected droplet size.

3. Environmental Test for a Driving Vehicle

To investigate the influence of FAD on combustion performance, the FAD was inserted into an old diesel vehicle and the PM, CO and NO_x were measured at an automobile inspection center operated by the Korean Road Traffic Safety Corporation. A test vehicle was operated at driving modes with five gear steps including as the idle, gear 2 at 30 km/h, gear 3 (60) at 60 km/h, gear 3 (80) at 80 km/h, gear 4 at 80 km/h, and gear 5 at 100 km/h.

3-1. Particulate Matter

Particulate matter emitted from diesel engines consists mainly of dry soot from the pyrolysis of hydrocarbon fuels at high tem-

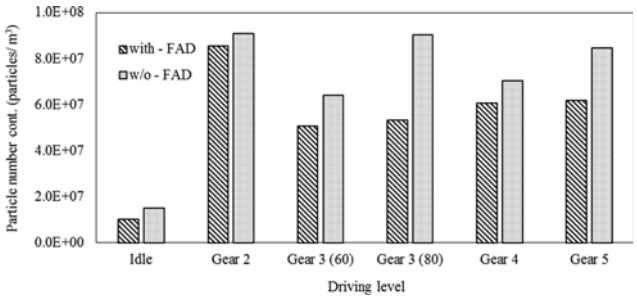

Fig. 11. Particle number concentration of PM_{10} for different driving mode.

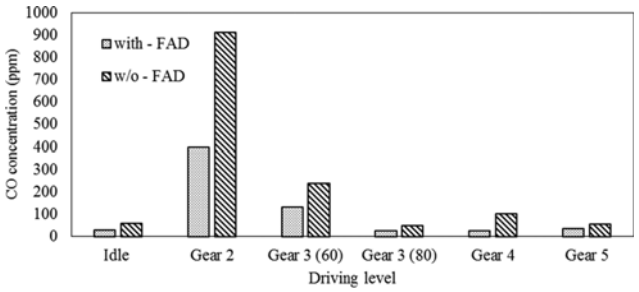

Fig. 13. Exhaust concentration of carbon monoxide with and without FAD for different driving condition.

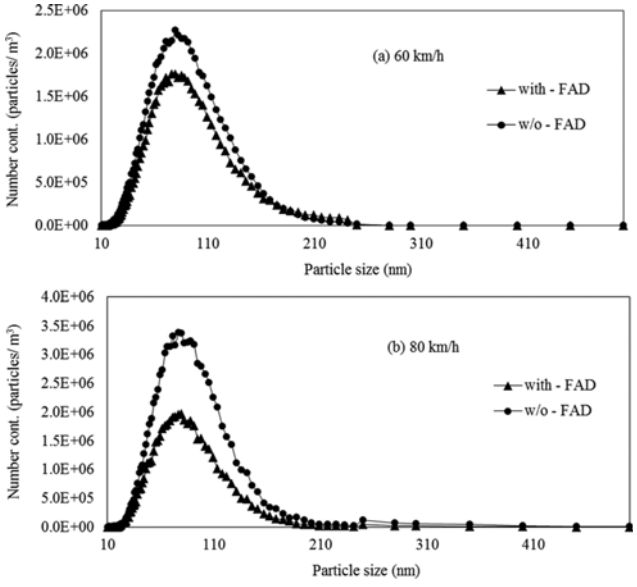

Fig. 12. Number based size distribution of exhausted PMs for gear 3 with and without FAD.

perature, a soluble organic fraction from unburned diesel and leaked lubricants, and trace amounts of salts such as sulfate [49]. Fine dust (represented as PM_{10}) contains various toxic and harmful substances. Fig. 11 shows the number concentrations of PM per cubic meter at different driving loads. The highest volume of fuel consumption was observed in gear 2. Gear 2 also showed the least benefit from the FAD. In contrast, the high speed load of gear 3 (80) showed a 42% PM_{10} reduction. The levels in gears 4 and 5 showed 13.5% and 26% PM_{10} reduction, respectively. The release of PM_{10} from the internal combustion of diesel cars was higher during driving than idle, and FAD played an important role in reducing PM in the exhaust.

Fig. 12 depicts the size distributions of the exhaust particulate matter for driving in gear 3 (60) and gear 3 (80). The fine particulates (less than 0.3 μm) were of primary interest in this work. As can be seen from Fig. 12(a) and (b), the fraction at a particular concentration and the absolute amount of exhausted particulate matters were lower with the FAD than without. Such an apparent reduction of PM exhausts is in accordance with a lower fuel consumption. For example, a higher mileage was observed with the FAD at 10.3 km/L rather than 10.1 km/L, without the FAD for gear 3 (80 km/h).

3-2. Gaseous Pollutants

The major gaseous pollutants emitted from automobiles in urban areas are nitrogen oxides (NO_x) and carbon monoxide (CO). The emission of gaseous pollutants depends on the driving condition and the efficiency of the internal engines. Carbon monoxide is produced as incomplete combustion happens, and its concentration depends on the ratio of the air/fuel mixture. Nitrogen oxides are formed while the chamber temperature is high enough for the reaction of nitrogen molecules with oxygen, so that the concentration of nitrogen oxides in the exhaust gas is associated with the combustion temperature, oxygen concentration and residence time in the chamber [50]. As can be seen from Fig. 13 and Table 5, the exhaust concentration of carbon monoxide was very low except in gears 2 and 3 (60). A release of 900 ppm CO was observed while driving the vehicle at 30 km/h in gear 2. However, the concentration of CO was reduced by approximately 50% with the FAD. Such a dramatic decrease might be due to the improved combustion efficiency and the lower fuel consumption. Fig. 13 also shows that FAD installation reduced the concentration of CO for all the driving levels. FAD obviously improves the combustion condition based on better mixing of fuel and air. The reduced carbon may convert to CO_2 and HC, which were not detected in this study. Nevertheless, FAD was more effective for carbon monoxide formation at a lower speed in Gear 2.

Nitrogen oxides were emitted over all the load levels as seen in Fig. 14. The highest concentration was detected (up to 280 ppm) in gear 4, but this value was lower than the general emissions from diesel engines of 500 ppm [51]. With FAD installation, more pro-

Table 5. Pollutant removal efficiency under different driving level after using FAD

Removal efficiency (%)	Idle	Gear 2	Gear 3 (60)	Gear 3 (80)	Gear 4	Gear 5
PM	31.48	5.95	21.00	40.91	14.01	27.00
CO	50.00	56.33	45.38	50.00	76.47	38.18
NO_x	2.78	18.18	13.42	7.69	3.81	4.55

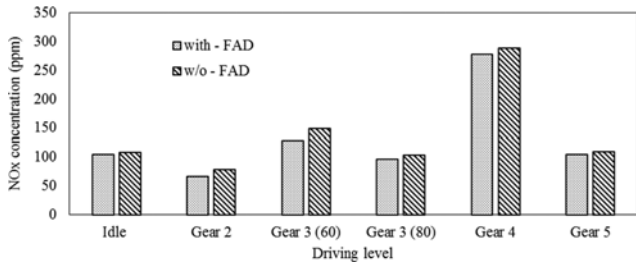

Fig. 14. Comparison of NO_x concentration in exhaust gas with and without FAD.

moted combustion of the fuel increased the temperature inside the cylinder chamber and the amount of oxygen also decreased. Therefore, the amount of thermal NO_x increased with the rise of the temperature. Meanwhile, high temperature impeded the formation of prompt and fuel-type NO_x. After the early period of combustion, the reduced amount of oxygen limited the further formation of NO_x. As a result, the quantity of NO_x was lower than that when FAD was not installed. FAD reduced the emissions of NO_x up to 13.4%. Nitrogen oxides are generally formed at high temperature under good combustion conditions. Thus, stable driving can still produce thermal NO_x. A slight decrease in NO_x emission was observed in all the levels except gear 2. This is due to the lower fuel consumption. The gear 2 results remained the same over five repeated runs, and likely reflect the unstable combustion conditions during low level driving.

3-3. Power Output and Fuel Consumption

The main purpose of the FAD is to enhance the atomization of fuel injection to the internal engine room. So, fuel consumption should be reduced due to the improved combustion efficiency while maintaining the required power. Therefore, the power as specified in rotations per minute (RPM) and fuel consumption rate were measured in this work (Figs. 15 and 16). Almost the same output power was observed for all driving levels with and without the FAD. The fuel consumptions required to achieve this output are compared in Fig. 16. Although less fuel was consumed for idling mode, the relative reduction rate was 26% on average. In addition, the reduction of fuel consumption by the FAD was 18% for gears 2 and 4, and 5% for gear 3 (60) and gear 3 (80), and 3% for gear 5. According to early references [17-19], systematically controlling atomization of the liquid fuel heavily influenced the combustion efficiency. Overall, the FAD showed higher performance and greater opportunities for energy savings and emission reduction utilizing the cavitation effect.

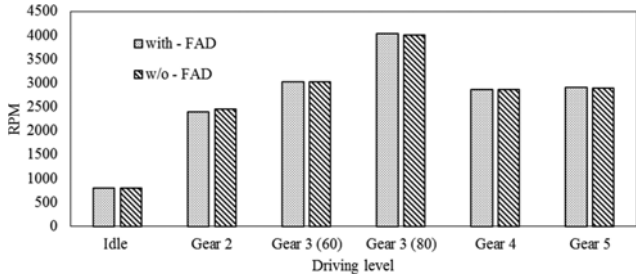

Fig. 15. RPMs of engine with and without FAD.

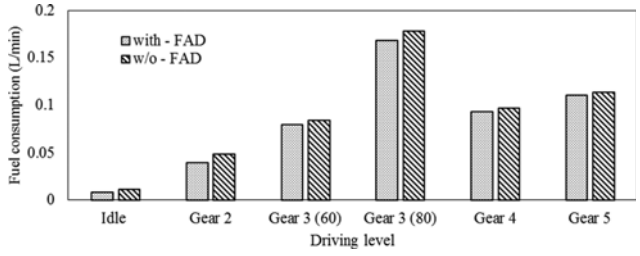

Fig. 16. Fuel consumption rate with and without FAD.

CONCLUSIONS

Cavitation is a vital factor in determining the fuel atomization performance and the combustion efficiency in an engine system. A new fuel activation device based on the cavitation effect was carefully investigated in terms of injected droplet size. A few conclusions from the lab and field tests were obtained as follows:

1) Regardless of nozzle type, the addition of an FAD enhanced the fuel spray along the axis of the flow path. More significant effects of the FAD were found closer to the nozzle. The effects of the FAD were more pronounced for the DM-1 and H7N nozzles, as SMD was reduced by 21.4% and 21.8%, respectively, while the J70 nozzle exhibited a maximum reduction of 3.93%.

2) The cumulative volume distribution curves further demonstrated the effects of FAD on the particle size.

3) The performance of a commercial nozzle (DM-1) was clearly improved using the FAD, which provided many fine droplets.

4) Driving a truck with an FAD resulted in less pollution with PM_{10}, CO and NO_x reductions of 42%, 50% and 13.4%, respectively. In addition, the reduction in fuel consumption ranged from 3% to 26%, depending on the driving conditions.

ACKNOWLEDGEMENTS

This work (NO. 20160951) was supported by the Business for Cooperative R&D between Industry, Academy, and Research Institute funded by the Korea Small and Medium Business Administration in 2016. Authors are grateful to Kyung Hee University for the assistance of an analytical instrument (KHU-20152127).

REFERENCES

1. N. Kumar and S. R. Chauhan, *J. Renew. Sustain. Energy Rev.*, **21**, 633 (2013).
2. J. M. Bergthorson and M. J. Thomson, *J. Renew. Sustain. Energy Rev.*, **42**, 1393 (2015).
3. N. Yilmaz, *Fuel*, **94**, 444 (2012).
4. W. Kim, The Seoul Institute Annual Research Digest 2016, The Seoul Institute, Seoul (2016).
5. S. Gupta, R. Poola and R. Sekar, *SAE Trans.*, **109**, 1713 (2000).
6. M. Talibi, P. Hellier, R. Balachandran and N. Ladommatos, *Int. J. Hydrogen Energy*, **39**, 15088 (2014).
7. J. Heywood, *Internal combustion engine fundamentals*, McGraw-

Hill, New York (1988).
8. F. Xing, A. Kumar, Y. Huang, S. N. Chan, C. Ruan, S. Gu and X. L. Fan, *Appl. Energy*, **193**, 28 (2017).
9. L. P. Bayvel, Liquid atomization, Taylor & Francis, Washington, D.C. (1993).
10. S. Sharma, R. Kumar, A. Chowdhury, Y. Yoon and S. Kumar, *Fuel*, **199**, 229 (2017).
11. W. Bergwerk, *Proc. Inst. Mech. Eng.*, **173**, 655 (1959).
12. J. Benajes, J. V. Pastor, R. Payri and A. H. Plazas, *J. Fluids Eng.*, **126**, 63 (2004).
13. R. Payri, J. M. Garcia, F. J. Salvador and J. Gimeno, *Fuel*, **84**, 551 (2005).
14. H. K. Suh, S. W. Park and C. S. Lee, *Fuel*, **86**, 2833 (2008).
15. C. E. Brennen, Cavitation and Bubble Dynamics, Oxford University Press, New York (1995).
16. W. H. Nurick, *J. Fluids Eng.*, **98**, 681 (1976).
17. A. Sou, M. I. Maulana, K. Isozaki and A. Tomiyama, *J. Fluid Sci. Technol.*, **3**, 622 (2008).
18. N. Tamaki, M. Shimizu, K. Nishida and H. Hiroyasu, *Atomization Sprays*, **8**, 179 (1998).
19. C. Soteriou, R. Andrews and M. Smith, *SAE Trans.*, **104**, 128 (1995).
20. S. I. Choi, J. P. Feng, H. S. Seo and Y. M. Jo, *J. Korean Soc. Atmos. Environ.*, **33**, 306 (2017).
21. C. Arcoumanis, H. Flora, M. Gavaises and M. Badami, *SAE Trans.*, **109**, 1485 (2000).
22. G. J. Jiang, Y. S. Zhang, H. Wen and G. Xiao, *Energy Convers. Manage.*, **103**, 208 (2015).
23. Y. Q. Gao, M. R. Wei, F. W. Yan, L. F. Chen, G. Z. Li and L. Y. Feng, *Exp. Therm. Fluid Sci.*, **87**, 69 (2017).
24. Z. X. He, Z. Y. Zhang, G. M. Guo, Q. Wang, X. Y. Leng and S. X. Sun, *Int. J. Heat Mass Transf.*, **78**, 13 (2016).
25. B. Carsten, Mixture Formation in Internal Combustion Engine, Springer Publications, New York and Berlin (2006).
26. L. L. Moyne, *Int. J. Spray Combust.*, **2**, 49 (2010).
27. F. J. Salvador, S. Ruiz, M. Crialesi-Esposito and I. Blanquer, *Int. J. Multiph. Flow*, **102**, 49 (2018).
28. M. Arai, Physics behind diesel sprays and its combustion, LAP Lambert Academic Publishing (2016).
29. M. Gavaises, A. Andriotis, D. Papoulias, N. Mitroglou and A. Theodorakakos, *Phys. Fluids*, **21**, 052107 (2009).
30. Z. X. He, W. J. Zhong, Q. Wang, Z. C. Jiang and Z. Shao, *Int. J. Therm. Sci.*, **70**, 132 (2013).
31. A. Sou, B. Biçer and A. Tomiyama, *Comput. Fluids*, **103**, 42 (2014).
32. Z. X. He, X. C. Tao, W. J. Zhong, X. Y. Leng, Q. Wang and P. Zhao, *Int. J. Heat Mass Transf.*, **65**, 117 (2015).
33. B. Bicer and A. Sou, *Appl. Math. Model.*, **40**, 4712 (2016).
34. B. Mohan, W. M. Yang and S. K. Chou, *Eng. Appl. Comp. Fluid*, **8**, 70 (2014).
35. D. Park, T. Lee, Y. Lee, W. Jeong, S. B. Kwon, D. Kim and K. Lee, *Sci. Total Environ.*, **575**, 97 (2017).
36. B. S. Prabhakar, S. P. Laxmanrao and K. J. A. M. Salim, *Int. J. Innov. Res. Sci. Eng. Technol.*, **2**, 6200 (2013).
37. Z. M. Wang, H. M. Xu, C. Z. Jiang and M. L. Wyszynski, *Fuel*, **174**, 140 (2016).
38. H. J. Kim, S. H. Park and C. S. Lee, *Fuel Process. Technol.*, **91**, 354 (2010).
39. D. L. Jing, F. Zhang, Y. F. Li, H. M. Xu and S. J. Shuai, *Fuel*, **199**, 478 (2017).
40. G. B. Li, J. M. Cao, M. L. Li, Y. H. Quan and Z. Y. Chen, *Fuel Process. Technol.*, **104**, 352 (2012).
41. R. J. Schick, General guidelines on drop size measurement techniques and terminology, 47th Chemical Processing Industry Exposition, New York (1997).
42. H. Hiroyasu, T. Kadota and M. Arai, *Bull. JSME*, **26**, 569 (1983).
43. G. M. Hidy, *J. Colloid Sci.*, **20**, 123 (1965).
44. A. Afshar, *Evaluation of liquid fuel spray models for hybrid RANS/lLES and DLES prediction of turbulent reactive flows*, University of Toronto, M.S. Thesis (2014).
45. H. K. Suh, S. H. Park and C. S. Lee, *Int. J. Automot. Technol.*, **9**, 217 (2008).
46. S. Lee and S. Park, *Fuel*, **137**, 50 (2014).
47. S. Huang, P. Deng, R. H. Huang, Z. W. Wang, Y. J. Ma and H. Dai, *Energy Convers. Manage.*, **106**, 911 (2015).
48. H. Hiroyasu, *Atomization Sprays*, **10**, 511 (2000).
49. K. K. Hendratna, O. Nishida, H. Fujita, W. Harano and D. H. Yoo, *Int. J. Res. Rev. Appl. Sci.*, **5**, 101 (2010).
50. İ. A. Reşitoğlu, K. Altinişik, and A. Keskin, *Clean Technol. Environ. Policy*, **17**, 15 (2015).
51. K. Azad, M. Rasul, B. Giannangelo and R. Islam, *Int. J. Automot. Mech. Eng.*, **12**, 2866 (2016).